

# Long-Lived Photon Blockade with Weak Optical Nonlinearity

You Wang,<sup>1,\*</sup> Xu Zheng,<sup>1,\*</sup> Timothy C. H. Liew,<sup>1,2,†</sup> and Y. D. Chong<sup>1,3,‡</sup>

<sup>1</sup>*Division of Physics and Applied Physics, School of Physical and Mathematical Sciences, Nanyang Technological University, Singapore 637371, Singapore*

<sup>2</sup>*MajuLab, International Joint Research Unit UMI 3654, CNRS, Université Côte d'Azur, Sorbonne Université,*

*National University of Singapore, Nanyang Technological University, Singapore*

<sup>3</sup>*Centre for Disruptive Photonic Technologies, School of Physical and Mathematical Sciences, Nanyang Technological University, Singapore 637371, Singapore*

In conventional photon blockade, the occupation of a cavity mode by more than one photon is suppressed via strong optical nonlinearity. An alternative, called unconventional photon blockade, can occur under weak nonlinearity by relying on quantum interference between fine-tuned cavities. A serious limitation is the very short antibunching time window, orders of magnitude less than the cavity lifetime. We present a method to achieve photon blockade over a large time window of several cavity lifetimes, even exceeding that of conventional photon blockade, while still requiring only weak nonlinearity. This “long-lived photon blockade” (LLPB) occurs when the single-photon Green’s function exhibits a zero at a large cavity loss rate, which is satisfied by an exemplary configuration of four coupled cavities under weak driving. Our analytical results agree well with wavefunction Monte Carlo simulations. The LLPB phenomenon may aid the development of single-photon sources utilizing materials with weak optical nonlinearities.

*Introduction*—Photon blockade is a quantum effect whereby one photon in a nonlinear resonator blocks the entry of other photons, giving rise to antibunched photon statistics [1–4]. Conventionally, photon blockade requires the optical nonlinearity within a cavity to exceed its loss: i.e.,  $\alpha \gg \gamma$ , where  $\alpha$  characterizes the strength of the nonlinearity and  $\gamma$  is the cavity decay rate. This can be interpreted in terms of a two-photon state being driven off-resonance by the nonlinearity, shifting its energy by more than the cavity linewidth [5–23]. Achieving this in the optical regime (including telecom wavelengths) is challenging, as material nonlinearities tend to be very weak relative to cavity linewidths. Systems featuring exceptionally strong optical nonlinearities are required, such as exciton-polaritons [24, 25], trions [26], Rydberg excitons [27], and Moire excitons [28].

The strong-nonlinearity condition may be bypassed via the phenomenon of unconventional photon blockade (UPB), which uses destructive interference between two or more nonlinear cavities (or cavity modes) to cancel the two-photon amplitudes [29–50]. It is commonly believed that UPB requires the inter-cavity coupling rate  $J$  to satisfy [29]

$$J \gg \gamma. \quad (1)$$

This seems to make intuitive sense: for interference to play a role, the photons must be able to hop many times before leaking away. In this regime, it then turns out that even a weak nonlinearity,  $\alpha \ll \gamma$ , can produce photon antibunching. However, even if the second-order photon

correlation  $g^{(2)}(\tau)$  vanishes at  $\tau = 0$ , the suppression only holds over a time window of

$$\delta\tau \sim 1/J \ll 1/\gamma, \quad (2)$$

due to the Rabi-like oscillations that  $J$  induces in the time-dependent state amplitudes. This is much smaller than the antibunching time window of  $\delta\tau \sim 1/\gamma$  for conventional photon blockade, and poses a serious practical obstacle to the realization and exploitation of UPB. For example, a proposal for UPB at telecom wavelengths [37] requires  $J \approx 20\gamma$  and yields an antibunching time window of  $\sim 100$  ps, around the resolution limit for current photodetectors. In such two-cavity models, the UPB condition reduces to  $\gamma^3 \propto \alpha J^2$ , implying that the cavity quality factors satisfy  $Q^3 \propto \omega_0^3 \delta\tau^2 / \alpha$ , where  $\omega_0$  is the cavity resonance frequency [31]. Given a lower bound on  $\delta\tau$  imposed by detector resolution limits, this condition sets a minimum requirement on  $Q$  that is unfavorable in the optical regime, where  $\omega_0$  is large and optical nonlinearities are typically weak. Flayac and Savona have suggested that with one-way dissipative inter-cavity couplings, the rapid oscillations in  $g^{(2)}(\tau)$  can be avoided [51]; however, such couplings are highly challenging to implement experimentally.

In this paper, we show that interference-assisted photon blockade does *not* require the strong-coupling condition (1), even with weakly nonlinear cavities and ordinary couplings. Using a Green’s function formalism, we analyze the steady-state behavior of coupled nonlinear cavities in the weak-driving regime [31], and show that antibunching solutions appear in the vicinity of 1-photon dark states, where the 1-photon Green’s function vanishes in a specific cavity. In the two-cavity systems where UPB was first discovered [29–31], as well as more complicated coupled-cavity configurations [50], such dark states occur only at  $\gamma = 0$ , giving rise to UPB solutions

\* These authors contributed equally to this work.

† timothy.liew@ntu.edu.sg

‡ yidong@ntu.edu.sg

with nonzero but small  $\gamma$  satisfying Eq. (1). However, certain coupled-cavity configurations host other families of dark states at large  $\gamma$  (relative to  $J$ ). We demonstrate this with a four-cavity system, showing that it produces a qualitatively different form of antibunching that we call long-lived photon blockade (LLPB). Unlike the earlier proposal involving one-way dissipative couplings [51], our four-cavity setup involves only standard (i.e., two-way and Hermitian) inter-cavity couplings. The antibunching condition  $g^{(2)}(0) = 0$  is satisfied alongside weak coupling ( $J \ll \gamma$ ) and weak nonlinearity ( $\alpha \ll \gamma$ ). Moreover,  $g^{(2)}(\tau)$  is suppressed over a time window  $\delta\tau \approx 8/\gamma$ , two orders of magnitude wider than a comparable two-cavity system exhibiting UPB, and even larger than for conventional photon blockade under strong nonlinearity. Thus, it may be possible to achieve photon blockade in the visible regime with weakly nonlinear optical media.

*Model*—We consider coupled nonlinear cavities, indexed by  $i = 1, \dots$ , under a weak coherent drive. Assuming for simplicity that all the cavities have identical parameters, the cavity Hamiltonian in the frame co-rotating with the driving field, excluding losses, is

$$\mathcal{H}_0 = \sum_{i \neq j} J_{ij} a_i^\dagger a_j + \sum_i \Delta a_i^\dagger a_i + \alpha \sum_i a_i^\dagger a_i^\dagger a_i a_i. \quad (3)$$

Here,  $\hbar = 1$ ,  $\Delta$  is the cavity detuning relative to the driving frequency,  $\alpha$  is the nonlinearity strength (Kerr coefficient),  $J_{ij}$  is the coupling between cavities  $i$  and  $j$ , and  $a_i$  is the photon annihilation operator for cavity  $i$ . We assume no magneto-optic activity, so  $J_{ij} = J_{ji} \in \mathbb{R}$  with a suitable gauge.

We assume a single-input, single-output setup where a cavity  $d$  is driven, and we look at the photon populations in a “readout” cavity (which may or may not be  $d$ ). The driving Hamiltonian is  $\mathcal{H}_d = F_d a_d^\dagger + F_d^* a_d$ , where  $F_d$  is the complex driving amplitude. (The following derivation can also be straightforwardly generalized to the case of multiple coherently driven cavities.) The density matrix  $\rho$  is then governed by the Lindblad master equation [52]

$$i \frac{d\rho}{dt} = [\mathcal{H}_0 + \mathcal{H}_d, \rho] + \frac{i\gamma}{2} \sum_i (2a_i \rho a_i^\dagger - a_i^\dagger a_i \rho - \rho a_i^\dagger a_i), \quad (4)$$

where the terms proportional to the cavity loss rate  $\gamma$  describe environmental noise. In the weak drive limit [31], stochastic quantum jumps—the first term in parentheses—can be ignored, and the problem reduces to a dissipative Schrödinger equation,

$$i \frac{d|\psi\rangle}{dt} = [\mathcal{H}(z) + \mathcal{H}_d] |\psi\rangle, \quad (5)$$

$$\mathcal{H}(z) \equiv \sum_{i \neq j} J_{ij} a_i^\dagger a_j + \sum_i z a_i^\dagger a_i + \alpha \sum_i a_i^\dagger a_i^\dagger a_i a_i, \quad (6)$$

$$z \equiv \Delta - i\gamma/2, \quad (7)$$

where the non-Hermitian effective Hamiltonian  $\mathcal{H}(z)$  is derived from (3) by adding loss to each site.

We seek a solution that is stationary (i.e., co-rotating with the drive,  $d/dt \rightarrow 0$ ). We truncate to superpositions of only 1- and 2-photon states, and derive the following expression for the equal-time second-order correlation function:

$$g_{ij}^{(2)} = \frac{\langle a_j^\dagger a_i^\dagger a_i a_j \rangle}{\langle a_j^\dagger a_j \rangle \langle a_i^\dagger a_i \rangle} = |f_{ij}(z)|^2, \quad (8)$$

$$f_{ij}(z) = \frac{\sqrt{2} \langle i, j | \bar{\psi}^{(2)} \rangle}{\langle i | \bar{\psi}^{(1)} \rangle \langle j | \bar{\psi}^{(1)} \rangle}, \quad (9)$$

where  $|i\rangle = a_i^\dagger |\text{vac}\rangle$  denotes the state with one photon in cavity  $i$  and  $|i, j\rangle \equiv |i\rangle \otimes |j\rangle$ . This generalizes a result reported by us for a specific lattice model [50]; the details of the derivation are given in the Supplemental Materials [53]. In Eq. (8), the expectation values are taken over the aforementioned stationary state, while in Eq. (9)  $|\bar{\psi}^{(1)}\rangle$  and  $|\bar{\psi}^{(2)}\rangle$  denote projections of the steady-state wavefunction to the 1- and 2-photon subspaces respectively.

Using Eq. (9), we can construct the following account of how photon antibunching arises. By fine-tuning the system parameters, it may be possible to satisfy  $\langle i | \bar{\psi}^{(1)} \rangle = 0$ , which we call a 1-photon dark state, for some cavity  $i$ . In the absence of nonlinearity, such a condition also implies a 2-photon dark state  $\langle i, j | \bar{\psi}^{(2)} \rangle = 0$ , since  $|\bar{\psi}^{(2)}\rangle = |\bar{\psi}^{(1)}\rangle \otimes |\bar{\psi}^{(1)}\rangle / \sqrt{2}$ . We then find that even though the numerator and denominator of (9) both vanish,  $f_{ij}(z)$  does not vanish; in fact,  $g_{ij}^{(2)} = 1$  for all  $z$ . A weak nonlinearity, however, can induce a small misalignment between the 1-photon and 2-photon dark states. Given a 1-photon dark state at  $z_0$ , the 2-photon dark state condition is shifted to a nearby value of  $z_0 + \delta z$ . At this point, the numerator of (9) vanishes while the denominator is nonzero. This is our desired photon antibunching point.

It is also helpful to introduce the 1-photon and non-interacting 2-photon Green’s functions,

$$G(z) \equiv \sum_n \frac{|\varphi_n\rangle \langle \varphi_n|}{z + \epsilon_n}, \quad (10)$$

$$G^{(2)}(z) \equiv \sum_{mn} \frac{|\varphi_m, \varphi_n\rangle \langle \varphi_m, \varphi_n|}{2z + \epsilon_m + \epsilon_n}, \quad (11)$$

where  $\{|\varphi_n\rangle\}$  is the eigenbasis of the coupling matrix,  $[J_{ij}] |\varphi_n\rangle = \epsilon_n |\varphi_n\rangle$ , and  $|\varphi_m, \varphi_n\rangle \equiv |\varphi_m\rangle \otimes |\varphi_n\rangle$ . Using these and assuming  $\alpha$  is perturbative, Eq. (9) can be expressed as

$$f_{ij}(z) = 1 - 2\alpha \sum_k \frac{G_{kd}^2}{G_{id} G_{jd}} \langle i, j | G^{(2)} | k, k \rangle. \quad (12)$$

The time-delayed correlation function  $g_{ij}^{(2)}(\tau)$  can be calculated by upgrading the  $a_i$ ’s and  $a_i^\dagger$ ’s to Heisenberg picture operators [53]. For  $\tau > 0$ , we find that the non-interacting 2-photon Green’s function in Eq. (12) is sim-

ply replaced by

$$G^{(2)}(z, \tau) \equiv e^{-iz\tau} \sum_{mn} \frac{|\varphi_m, \varphi_n\rangle \langle \varphi_m, \varphi_n|}{2z + \epsilon_m + \epsilon_n} e^{-i\epsilon_n \tau}. \quad (13)$$

This analytical form of  $g_{ij}^{(2)}(\tau)$  has not previously been reported, to our knowledge. Below, we will use it to revisit UPB, and then demonstrate the LLPB phenomenon.

*Conventional blockade*—First, let us consider photon blockade in one cavity. In this case, we can bypass the above perturbative procedure and directly find the Green's functions, obtaining [53]

$$g_{11}^{(2)}(\tau) = \frac{1}{1 + 4\alpha^2/\gamma^2} + \frac{4\alpha^2/\gamma^2}{1 + 4\alpha^2/\gamma^2} \left(1 - e^{-\frac{\gamma}{2}\tau}\right)^2. \quad (14)$$

The condition  $g_{11}^{(2)}(0) \approx 0$  requires  $\alpha \gg \gamma$ . The corresponding time window, estimated as the interval over which  $g^{(2)}(\tau) < 0.5$ , is  $\delta\tau = -4\ln(1 - \sqrt{0.5})/\gamma \approx 5/\gamma$ .

*UPB with two cavities*—For a two-cavity system, with  $J_{12} = J_{21} = J \in \mathbb{R}^+$ , the coupling matrix has eigenvalues  $\epsilon_{1,2} = \pm J$  and the eigenbasis  $|\varphi_{1,2}\rangle = 2^{-1/2}(|1\rangle \pm |2\rangle)$ . Eqs. (10)–(12) predict antibunching in the driven cavity ( $d = 1$ ),  $g_{11}^{(2)}(0) = 0$ , if and only if  $z^3 \approx -\alpha J^2/2$  [53]. The three roots correspond to three 2-photon dark states, and are depicted by blue circles in Fig. 1(a). They lie close to the 1-photon dark state at  $z = 0$ , for which  $\langle 1|\bar{\psi}^{(1)}\rangle \propto G_{11} = z(z^2 - J^2)^{-1} = 0$ , as indicated by the red cross in the figure. We focus on the root with positive cavity loss, for which

$$\gamma = \sqrt{3}\Delta \propto J\sqrt{\alpha/\gamma}. \quad (15)$$

Unlike the one-cavity case, this is achievable for  $\alpha \ll \gamma$ , but only if we enter the strong-coupling regime (1), as previously noted [29, 31]. Moreover, from Eq. (13),

$$g_{11}^{(2)}(\tau) \approx \left(1 - e^{-\frac{\gamma}{2}\tau} \cos(\Delta\tau) \cos(J\tau)\right)^2. \quad (16)$$

The fast oscillation in  $\cos(J\tau)$  yields a small time window of  $\delta\tau \sim 1/J$ , tied to the large coupling eigenvalues  $\pm J$ .

Photon antibunching in this model follows the mechanism laid out by Eqs. (8)–(12). The 2-photon dark state is perturbed away from the 1-photon dark state, and since the latter occurs at  $z = 0$ , the solution we arrive at involves small  $\gamma$  (relative to  $J$ ). The lattice model studied in Ref. 50 also works similarly.

*Long-Lived Photon Blockade*—The above scenario can be bypassed if we find a configuration of cavities with a 1-photon dark state at large  $\gamma$ . Specifically, we want the *linear* single-photon Green's function to satisfy  $G_{id}(z) = 0$  for some  $i, d$ , with  $\gamma = -2\text{Im}(z) \gg \max |J_{ij}|$ . This turns out to be impossible for  $N = 2$  and  $N = 3$  (though if we relax the assumption that the cavities are identical, we can find a zero for  $N = 3$  if one cavity is completely lossless); for details, see the Supplemental Materials [53]. For  $N = 4$ , however, the condition can be satisfied.

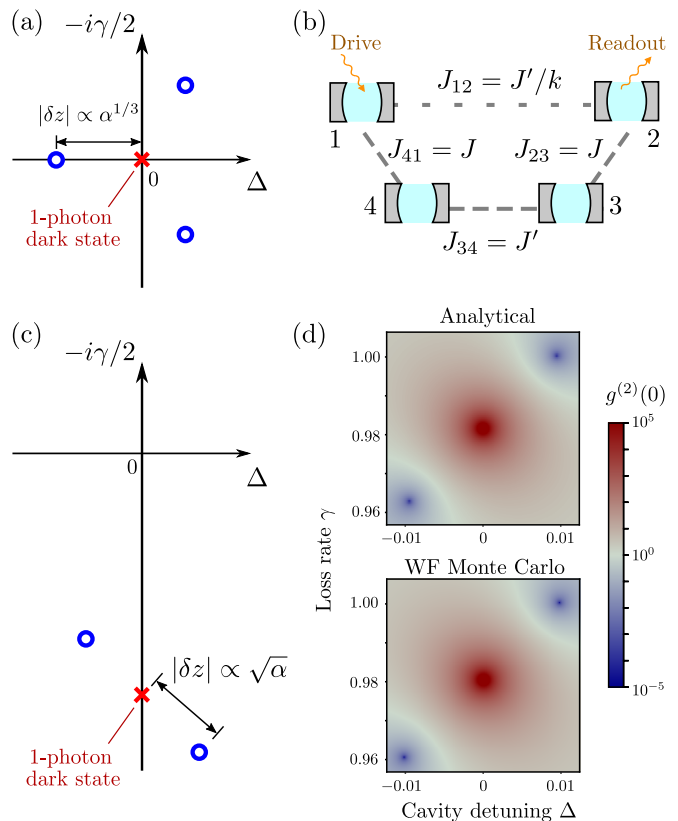


FIG. 1. (a) Schematic of the zeros (circles) and pole (cross) of  $f_{11}(z)$  in the complex  $z$  plane, for a two-cavity model. The pole occurs at  $z = 0$ , and UPB occurs at the zeros. (b) Schematic of a four-cavity setup that can exhibit long-lived photon blockade (LLPB). (c) Distribution of zeros (circles) and pole (cross) of  $f_{22}(z)$  for the four-cavity model of (b). This illustration is not drawn to scale. (d) Equal-time two-photon correlation function  $g^{(2)}(0)$  for the four-cavity system versus cavity detuning  $\Delta$  and loss rate  $\gamma$ . Upper plot: analytical results obtained from Eqs. (20)–(22). Near the pole (central red spot), there are two zeros of  $g^{(2)}(0)$  (blue spots) corresponding to LLPB. The model parameters are  $k = 16$ ,  $J = 0.1227$ ,  $J' = 0.02454$ , and  $\alpha = 0.001227$ , chosen so that one of the LLPB points occurs at  $\gamma = 1$ . Lower plot: WFMC simulation results, obtained by directly solving Lindblad master equation with the same parameters and  $F_d = 10^{-5}$ .

Consider the configuration shown in Fig. 1(b), with four cavities arranged in a ring with couplings  $J_{12}, J_{23}, J_{34}, J_{41} \in \mathbb{R}^+$ ; the driven cavity is  $d = 1$ , and photons are extracted from cavity  $i = 2$ . A Dyson series expansion in the weak-coupling regime [54] indicates that  $G_{12}(z) = G_{21}(z)$  can have a zero that meets the above conditions if  $J_{12} \ll J_{23}, J_{34}, J_{41}$ . Specifically, we consider

$$[J_{ij}] = \begin{pmatrix} 0 & J'/k & 0 & J \\ J'/k & 0 & J & 0 \\ 0 & J & 0 & J' \\ J & 0 & J' & 0 \end{pmatrix}, \quad (17)$$

where  $k \gg 1$ . Using Eqs. (6) and (10),

$$G_{21}(z) = -\frac{J'}{k}(z+z_0)(z-z_0)/\det \mathcal{H}, \quad (18)$$

$$z_0 \equiv -iJ\sqrt{k - (J'/J)^2}. \quad (19)$$

At  $z = z_0$ ,  $G_{21}$  has a zero and hence  $f_{22}$  has a pole (we ignore  $z = -z_0$ , which involves putting gain in the cavities). From Eqs. (7) and (19), we have  $\Delta = 0$  and  $\gamma \approx 2\sqrt{k}J$ , consistent with the weak-coupling regime.

Next, we search near  $z_0$  for a zero of  $f_{22}(z)$ . Substituting Eq. (18) back into Eq. (12), we find that for  $z \approx z_0$ ,

$$f(z) \approx \frac{(z - z_0 - \delta z)(z - z_0 + \delta z)}{(z - z_0)^2}, \quad (20)$$

$$\delta z^2 = -\frac{k^2\alpha}{2z_0^2 J'^2} \left[ \sum_i G_{22ii}^{(2)} (G_{i1} \cdot \det \mathcal{H})^2 \right]_{z=z_0} \quad (21)$$

where  $G_{22ii}^{(2)} \equiv \langle 2, 2 | G^{(2)}(z) | i, i \rangle$ . By further assuming  $J \gg J'$ , it is approximated as [53]

$$\delta z \approx \pm \frac{\sqrt{38}}{16} \sqrt{\alpha\gamma} e^{-i\pi/4}. \quad (22)$$

LLPB is predicted to occur at  $z \approx z_0 \pm \delta z$ , as shown schematically in Fig. 1(c).

In the upper plot of Fig. 1(d), we plot  $g_{22}^{(2)}(0)$  versus the cavity parameters  $\Delta$  and  $\gamma$  using Eqs. (20)–(22). The parameters, stated in the figure caption, satisfy  $\alpha \ll \gamma$  (weak nonlinearity) and  $J'/k \ll J' \ll J \ll \gamma$  (weak coupling). For comparison, the lower plot of Fig. 1(d) shows the results obtained based on wavefunction Monte Carlo (WFMC) [55–58] simulations, which directly solve the Lindblad master equation (4) using  $F_d = 10^{-5}$ , with all other parameters kept the same. It is worth noting that the WFMC simulations give  $g_{22}^{(2)}(0) \ll 1$ , but not exactly zero, in the weak-drive regime. This value of  $g_{22}^{(2)}(0)$  increases with  $F_d$ , alongside an increase in the mean photon occupation number in the signal cavity [53].

*Antibunching time window*—In Fig. 2, the green curve shows the time-delayed second-order correlation function  $g^{(2)}(\tau)$  for the above four-cavity system, at one of its LLPB points (at  $\gamma = 1$ ). The photon antibunching time window is approximately  $8/\gamma$ . This plot is obtained from WFMC simulations, but the analytical theory gives almost identical results. The analytic approximation for this result can be derived for  $J' \ll J$  by approximating the eigenvalues and eigenvectors of the coupling Hamiltonian to second order in  $J'$ . The full result is given in Supplemental Materials [53]. If we look into the short time scale  $\tau \sim 1/\gamma$  and expand  $g_{22}^{(2)}(\tau)$  as polynomial of  $\gamma\tau$ , assuming negligible  $\alpha$ , we find

$$g_{22}^{(2)}(\tau) \approx (\gamma\tau)^4/64. \quad (23)$$

This small  $\tau$  expansion is order-4 and fundamentally distinct from the quadratic conventional photon blockade case  $g^{(2)}(\tau) \approx (\gamma\tau)^2/4$ , by Eq. (14).

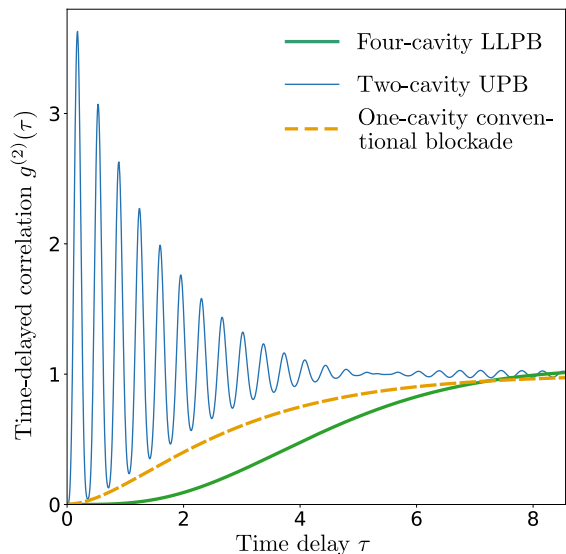


FIG. 2. Time-delayed second-order correlation function  $g^{(2)}(\tau)$  for a four-cavity system with LLPB (green curve), a two-cavity system with UPB (blue curve), and a one-cavity system with conventional photon blockade (orange dashes). All results are obtained using WFMC simulations. The model parameters for the four-cavity LLPB setup are the same as in Fig. 1, with  $\Delta = 0.009571$  and  $\gamma = 1$ . The other two cases are tuned for photon blockade at the same  $\gamma$ . For the two-cavity system, we choose the same nonlinearity strength  $\alpha = 0.001227$ , for which UPB occurs at  $J \approx 17.67$  and  $\Delta \approx 0.2915$ . For the one-cavity system, we set  $\alpha = 10$  and  $\Delta = 0.02491$ .

For comparison, the blue curve in Fig. 2 shows  $g^{(2)}(\tau)$  for a comparable two-cavity UPB setup [29]. Here we take  $\alpha = 0.001227$ , the same as in the four-cavity LLPB case. For the same decay rate  $\gamma = 1$ , two-cavity UPB is achieved for  $J \approx 17.67$ , and the strong coupling results in rapid oscillations of  $g^{(2)}(\tau)$ . The central antibunching window, estimated as the window over which  $g^{(2)}(\tau) < 0.5$ , is around 90 times smaller than in the LLPB case.

As a further comparison, the orange dashes in Fig. 2 show  $g^{(2)}(\tau)$  for a one-cavity setup with  $\gamma = 1$  and  $\alpha = 10$ . (Note that  $g^{(2)}(0)$  does not reach precisely zero under conventional photon blockade; we simply choose  $\alpha$  so that it is visibly suppressed.) The  $g^{(2)}(\tau)$  curves for both LLPB and conventional photon blockade have no oscillations, unlike the two-cavity UPB case. Remarkably, the LLPB curve has a significantly flatter bottom near  $\tau = 0$  than the curve for conventional photon blockade, and the time window is larger by a factor of around 1.68. This can be understood from Eq. (23); the expansion leading term is of order-4 in  $\gamma\tau$ , approximately  $(\gamma\tau)^4/64$ , compared to the quadratic term  $\approx (\gamma\tau)^2/4$  for the single-cavity case. This characteristic results in a more gradual change in the dip, which may be advantageous for pulsed device operations [37, 39].

*Conclusion*—We have re-analyzed the origins of unconventional photon blockade (UPB), in which photon

antibunching is achieved by quantum interference in weakly nonlinear coupled cavities [29]. A major problem with UPB has hitherto been the rapid oscillation in  $g^{(2)}(\tau)$  due to strong inter-cavity coupling [37, 39]. We show that this can be overcome by designing a coupled-cavity system so that the linear single-photon Green's function exhibits a zero (a 1-photon dark state) at a large cavity loss rate. This leads to a “long-lived photon blockade” (LLPB) scenario whereby  $g^{(2)}(\tau) \propto \tau^4$  and the time window exceeds that of conventional photon blockade under strong nonlinearity. It is remarkable that *shortening* the cavity lifetime can effectively *lengthen* the antibunching time window, which can be regarded as a fresh example of non-Hermiticity (in the form of dissipation) producing unexpected physical behaviors [59, 60]. Our

proposal does not need one-way inter-cavity couplings or other exotic requirements [39, 51], and should be highly compatible with quantum optics experiments.

Our theoretical framework offers ample scope for further generalization and optimization. For instance, in the four-cavity configuration of Fig. 1(b), the couplings are described by just three parameters for simplicity, but they can instead be individually optimized to achieve an even larger  $g^{(2)}(\tau)$  time window. Coherently driving multiple cavities also offers additional possibilities for achieving LLPB with other cavity configurations. Possible implementation challenges may include the need for fine-tuning and ensuring the stability of the inter-cavity couplings and other system parameters, which is a problem shared with the original UPB setup and all other related schemes to date.

- 
- [1] L. Tian and H. J. Carmichael, Quantum trajectory simulations of two-state behavior in an optical cavity containing one atom, *Phys. Rev. A* **46**, R6801 (1992).
- [2] W. Leoński and R. Tanaś, Possibility of producing the one-photon state in a kicked cavity with a nonlinear Kerr medium, *Phys. Rev. A* **49**, R20 (1994).
- [3] A. Imamoğlu, H. Schmidt, G. Woods, and M. Deutsch, Strongly interacting photons in a nonlinear cavity, *Phys. Rev. Lett.* **79**, 1467 (1997).
- [4] P. Lodahl, S. Mahmoodian, and S. Stobbe, Interfacing single photons and single quantum dots with photonic nanostructures, *Rev. Mod. Phys.* **87**, 347 (2015).
- [5] K. M. Birnbaum, A. Boca, R. Miller, A. D. Boozer, T. E. Northup, and H. J. Kimble, Photon blockade in an optical cavity with one trapped atom, *Nature* **436**, 87 (2005).
- [6] B. Dayan, A. S. Parkins, T. Aoki, E. P. Ostby, K. J. Vahala, and H. J. Kimble, A photon turnstile dynamically regulated by one atom, *Science* **319**, 1062 (2008).
- [7] C. Hamsen, K. N. Tolazzi, T. Wilk, and G. Rempe, Two-photon blockade in an atom-driven cavity QED system, *Phys. Rev. Lett.* **118**, 133604 (2017).
- [8] P. Michler, A. Kiraz, C. Becher, W. V. Schoenfeld, P. M. Petroff, L. Zhang, E. Hu, and A. Imamoğlu, A quantum dot single-photon turnstile device, *Science* **290**, 2282 (2000).
- [9] A. Faraon, I. Fushman, D. Englund, N. Stoltz, P. Petroff, and J. Vučković, Coherent generation of non-classical light on a chip via photon-induced tunnelling and blockade, *Nat. Phys.* **4**, 859 (2008).
- [10] J. Claudon, J. Bleuse, N. S. Malik, M. Bazin, P. Jaffrennou, N. Gregersen, C. Sauvan, P. Lalanne, and J.-M. Gérard, A highly efficient single-photon source based on a quantum dot in a photonic nanowire, *Nat. Photon.* **4**, 174 (2010).
- [11] Y.-M. He, Y. He, Y.-J. Wei, D. Wu, M. Atatüre, C. Schneider, S. Höfling, M. Kamp, C.-Y. Lu, and J.-W. Pan, On-demand semiconductor single-photon source with near-unity indistinguishability, *Nat. Nanotech.* **8**, 213 (2013).
- [12] K. H. Madsen, S. Ates, J. Liu, A. Javadi, S. M. Albrecht, I. Yeo, S. Stobbe, and P. Lodahl, Efficient out-coupling of high-purity single photons from a coherent quantum dot in a photonic-crystal cavity, *Phys. Rev. B* **90**, 155303 (2014).
- [13] M. Gschrey, A. Thoma, P. Schnauber, M. Seifried, R. Schmidt, B. Wohlfeil, L. Krüger, J. H. Schulze, T. Heindel, S. Burger, F. Schmidt, A. Strittmatter, S. Rodt, and S. Reitzenstein, Highly indistinguishable photons from deterministic quantum-dot microlenses utilizing three-dimensional in situ electron-beam lithography, *Nat. Comm.* **6**, 7662 (2015).
- [14] N. Somaschi, V. Giesz, L. D. Santis, J. C. Loredó, M. P. Almeida, G. Hornecker, S. L. Portalupi, T. Grange, C. Antón, J. Demory, C. Gómez, I. Sagnes, N. D. Lanzillotti-Kimura, A. Lemaître, A. Auffeves, A. G. White, L. Lanco, and P. Senellart, Near-optimal single-photon sources in the solid state, *Nature Photonics* **10**, 340 (2016).
- [15] C. Dory, K. A. Fischer, K. Müller, K. G. Lagoudakis, T. Sarmiento, A. Rundquist, J. L. Zhang, Y. Kelaita, N. V. Sapra, and J. Vučković, Tuning the photon statistics of a strongly coupled nanophotonic system, *Phys. Rev. A* **95**, 023804 (2017).
- [16] N. Jia, N. Schine, A. Georgakopoulos, A. Ryou, L. W. Clark, A. Sommer, and J. Simon, A strongly interacting polaritonic quantum dot, *Nat. Phys.* **14**, 550 (2018).
- [17] C. Lang, D. Bozyigit, C. Eichler, L. Steffen, J. M. Fink, A. A. Abdumalikov, M. Baur, S. Filipp, M. P. da Silva, A. Blais, and A. Wallraff, Observation of resonant photon blockade at microwave frequencies using correlation function measurements, *Phys. Rev. Lett.* **106**, 243601 (2011).
- [18] X. Wang, A. Miranowicz, H.-R. Li, and F. Nori, Multiple-output microwave single-photon source using superconducting circuits with longitudinal and transverse couplings, *Phys. Rev. A* **94**, 053858 (2016).
- [19] P. Rabl, Photon blockade effect in optomechanical systems, *Phys. Rev. Lett.* **107**, 063601 (2011).
- [20] X.-W. Xu, A.-X. Chen, and Y.-x. Liu, Phonon blockade in a nanomechanical resonator resonantly coupled to a qubit, *Phys. Rev. A* **94**, 063853 (2016).
- [21] M.-A. Lemonde, N. Didier, and A. A. Clerk, Enhanced nonlinear interactions in quantum optomechanics via mechanical amplification, *Nat. Comm.* **7**, 11338 (2016).
- [22] A. Majumdar, M. Bajcsy, A. Rundquist, and J. Vučković,

- Loss-enabled sub-poissonian light generation in a bimodal nanocavity, *Phys. Rev. Lett.* **108**, 183601 (2012).
- [23] A. Majumdar and D. Gerace, Single-photon blockade in doubly resonant nanocavities with second-order nonlinearity, *Phys. Rev. B* **87**, 235319 (2013).
- [24] A. Delteil, T. Fink, A. Schade, S. Höfling, C. Schneider, and A. İmamoğlu, Towards polariton blockade of confined exciton-polaritons, *Nature Materials* **18**, 219–222 (2019).
- [25] G. Muñoz-Matutano, A. Wood, M. Johnsson, X. Vidal, B. Q. Baragiola, A. Reinhard, A. Lemaître, J. Bloch, A. Amo, G. Nogues, B. Besga, M. Richard, and T. Volz, Emergence of quantum correlations from interacting fibre-cavity polaritons, *Nature Materials* **18**, 213–218 (2019).
- [26] O. Kyriienko, D. N. Krizhanovskii, and I. A. Shelykh, Nonlinear quantum optics with trion polaritons in 2d monolayers: Conventional and unconventional photon blockade, *Phys. Rev. Lett.* **125**, 197402 (2020).
- [27] K. Orfanakis, S. K. Rajendran, V. Walther, T. Volz, T. Pohl, and H. Ohadi, Rydberg exciton-polaritons in a Cu2O microcavity, *Nature Materials* **21**, 767–772 (2022).
- [28] L. Zhang, F. Wu, S. Hou, Z. Zhang, Y.-H. Chou, K. Watanabe, T. Taniguchi, S. R. Forrest, and H. Deng, Van der Waals heterostructure polaritons with Moiré-induced nonlinearity, *Nature* **591**, 61–65 (2021).
- [29] T. C. H. Liew and V. Savona, Single photons from coupled quantum modes, *Phys. Rev. Lett.* **104**, 183601 (2010).
- [30] S. Ferretti, L. C. Andreani, H. E. Türeci, and D. Gerace, Photon correlations in a two-site nonlinear cavity system under coherent drive and dissipation, *Phys. Rev. A* **82**, 013841 (2010).
- [31] M. Bamba, A. İmamoğlu, I. Carusotto, and C. Ciuti, Origin of strong photon antibunching in weakly nonlinear photonic molecules, *Phys. Rev. A* **83**, 021802(R) (2011).
- [32] M. Bamba and C. Ciuti, Counter-polarized single-photon generation from the auxiliary cavity of a weakly nonlinear photonic molecule, *Appl. Phys. Lett.* **99**, 171111 (2011).
- [33] H. Flayac and V. Savona, Input-output theory of the unconventional photon blockade, *Phys. Rev. A* **88**, 033836 (2013).
- [34] X.-W. Xu and Y. Li, Strong photon antibunching of symmetric and antisymmetric modes in weakly nonlinear photonic molecules, *Phys. Rev. A* **90**, 033809 (2014).
- [35] M.-A. Lemonde, N. Didier, and A. A. Clerk, Antibunching and unconventional photon blockade with Gaussian squeezed states, *Phys. Rev. A* **90**, 063824 (2014).
- [36] D. Gerace and V. Savona, Unconventional photon blockade in doubly resonant microcavities with second-order nonlinearity, *Phys. Rev. A* **89**, 031803(R) (2014).
- [37] H. Flayac, D. Gerace, and V. Savona, An all-silicon single-photon source by unconventional photon blockade, *Scientific Reports* **5**, 11223 (2015).
- [38] H. Z. Shen, Y. H. Zhou, and X. X. Yi, Tunable photon blockade in coupled semiconductor cavities, *Phys. Rev. A* **91**, 063808 (2015).
- [39] H. Flayac and V. Savona, Unconventional photon blockade, *Phys. Rev. A* **96**, 053810 (2017).
- [40] G. Wang, H. Z. Shen, C. Sun, C. Wu, J.-L. Chen, and K. Xue, Unconventional photon blockade in weakly nonlinear photonic molecules with bilateral drive, *Journal of Modern Optics* **64**, 583 (2017).
- [41] B. Sarma and A. K. Sarma, Quantum-interference-assisted photon blockade in a cavity via parametric interactions, *Phys. Rev. A* **96**, 053827 (2017).
- [42] S. Ghosh and T. C. H. Liew, Single photons from a gain medium below threshold, *Phys. Rev. B* **97**, 241301(R) (2018).
- [43] H. Z. Shen, S. Xu, Y. H. Zhou, G. Wang, and X. X. Yi, Unconventional photon blockade from bimodal driving and dissipations in coupled semiconductor microcavities, *Journal of Physics B: Atomic, Molecular and Optical Physics* **51**, 035503 (2018).
- [44] B. Sarma and A. K. Sarma, Unconventional photon blockade in three-mode optomechanics, *Phys. Rev. A* **98**, 013826 (2018).
- [45] S. Ghosh and T. C. H. Liew, Dynamical blockade in a single-mode Bosonic system, *Phys. Rev. Lett.* **123**, 013602 (2019).
- [46] H. Carmichael, R. Brecha, and P. Rice, Quantum interference and collapse of the wavefunction in cavity QED, *Optics Communications* **82**, 73 (1991).
- [47] M. Radulaski, K. A. Fischer, K. G. Lagoudakis, J. L. Zhang, and J. Vučković, Photon blockade in two-emitter-cavity systems, *Phys. Rev. A* **96**, 011801(R) (2017).
- [48] K. Kamide, Y. Ota, S. Iwamoto, and Y. Arakawa, Method for generating a photonic NOON state with quantum dots in coupled nanocavities, *Phys. Rev. A* **96**, 013853 (2017).
- [49] E. Zubizarreta Casalengua, J. C. López Carreño, F. P. Laussy, and E. d. Valle, Conventional and unconventional photon statistics, *Laser & Photonics Reviews* **14**, 1900279 (2020).
- [50] Y. Wang, W. Verstraelen, B. Zhang, T. C. H. Liew, and Y. D. Chong, Giant enhancement of unconventional photon blockade in a dimer chain, *Phys. Rev. Lett.* **127**, 240402 (2021).
- [51] H. Flayac and V. Savona, Single photons from dissipation in coupled cavities, *Phys. Rev. A* **94**, 013815 (2016).
- [52] H. Breuer and F. Petruccione, *The Theory of Open Quantum Systems* (OUP Oxford, 2007).
- [53] See supplementary material.
- [54] A. A. Clerk, Introduction to quantum non-reciprocal interactions: from non-Hermitian Hamiltonians to quantum master equations and quantum feedforward schemes, *SciPost Phys. Lect. Notes* , 44 (2022).
- [55] R. Dum, A. S. Parkins, P. Zoller, and C. W. Gardiner, Monte Carlo simulation of master equations in quantum optics for vacuum, thermal, and squeezed reservoirs, *Phys. Rev. A* **46**, 4382 (1992).
- [56] K. Mølmer, Y. Castin, and J. Dalibard, Monte Carlo wave-function method in quantum optics, *J. Opt. Soc. Am. B* **10**, 524 (1993).
- [57] H. Carmichael, *An open systems approach to quantum optics* (Springer, 1993).
- [58] A. Barchielli and V. P. Belavkin, Measurements continuous in time and a posteriori states in quantum mechanics, *Journal of Physics A: Mathematical and General* **24**, 1495 (1991).
- [59] C. M. Bender, Making sense of non-hermitian hamiltonians, *Reports on Progress in Physics* **70**, 947 (2007).
- [60] Y. Ashida, Z. Gong, and M. Ueda, Non-hermitian physics, *Advances in Physics* **69**, 249 (2020).
- [61] H. Z. Shen, Y. H. Zhou, and X. X. Yi, Quantum optical diode with semiconductor microcavities, *Phys. Rev. A* **90**, 023849 (2014).

## Supplemental Materials

### S1. DERIVATION OF DELAYED SECOND-ORDER CORRELATIONS UNDER WEAK DRIVING

As mentioned in the main text, the steady state for a system of driven nonlinear cavities, in the limit where the driving is weak, can be obtained from a dissipative effective Schrödinger equation. Following Ref. [31], under the weak-driving assumption the Hilbert space is divided into subspaces of different photon number, and the wavefunction is written as a superposition of contributions from each subspace:

$$|\psi\rangle = |\psi^{(0)}\rangle + |\psi^{(1)}\rangle + |\psi^{(2)}\rangle + \dots \quad (\text{S1})$$

Under weak driving, the amplitudes in higher photon number subspaces should be negligible. Hence, we solve the Schrödinger equation for each subspace recursively [31], truncating at a given photon number bound:

$$\begin{aligned} i\frac{d}{dt}|\psi^{(k)}\rangle &= \mathcal{H}|\psi^{(k)}\rangle + F_d a_d^\dagger |\psi^{(k-1)}\rangle + F_d^* a_d |\psi^{(k+1)}\rangle \\ &\approx \mathcal{H}|\psi^{(k)}\rangle + F_d a_d^\dagger |\psi^{(k-1)}\rangle. \end{aligned} \quad (\text{S2})$$

The steady-state wavefunction  $|\bar{\psi}\rangle$  can be found by setting the time derivative in each subspace to zero. We obtain

$$|\bar{\psi}^{(k)}\rangle = -F_d \mathcal{H}^{-1} a_d^\dagger |\bar{\psi}^{(k-1)}\rangle, \quad (\text{S3})$$

with  $|\bar{\psi}^{(0)}\rangle = |\psi^{(0)}\rangle$  being the vacuum state.

For the single-photon subspace, the effective Hamiltonian is  $\mathcal{H} = [J_{ij}] + z\mathcal{L}$ . This subspace is spanned by the eigenvectors of the coupling matrix, i.e.,

$$[J_{ij}]|\varphi_n\rangle = \epsilon_n |\varphi_n\rangle. \quad (\text{S4})$$

Supposing that one cavity  $d$  is driven, (S3) reduces to

$$|\bar{\psi}^{(1)}\rangle = -F_d G|d\rangle, \quad \text{where } G \equiv \mathcal{H}^{-1} = \sum_n \frac{|\varphi_n\rangle\langle\varphi_n|}{z + \epsilon_n}. \quad (\text{S5})$$

In this work, we truncate the calculation at two photons. For the 2-photon subspace, we use the basis formed by tensor products  $|\varphi_{mn}\rangle = |\varphi_m\rangle \otimes |\varphi_n\rangle$ . We then calculate the steady-state amplitude in this subspace using a perturbation expansion to first order in the nonlinearity strength  $\alpha$  [50]:

$$\begin{aligned} |\bar{\psi}^{(2)}\rangle &\approx |\bar{\psi}_0^{(2)}\rangle + \alpha |\bar{\psi}_1^{(2)}\rangle \\ &= \frac{1}{\sqrt{2}} |\bar{\psi}^{(1)}\rangle \otimes |\bar{\psi}^{(1)}\rangle - \sqrt{2}\alpha F_d^2 \sum_k G_{kd}^2 G^{(2)}|k, k\rangle, \end{aligned} \quad (\text{S6})$$

where  $G_{kd} \equiv \langle k|G|d\rangle$  is the  $k, d$  element of the single-photon Green's function and

$$G^{(2)} \equiv \sum_{mn} \frac{|\varphi_{nm}\rangle\langle\varphi_{mn}|}{2z + \epsilon_m + \epsilon_n} \quad (\text{S7})$$

is the linear two-photon Green's function.

The second-order correlation function between sites  $i$  and  $j$ , with time delay  $\tau \geq 0$ , is defined as

$$g_{ij}^{(2)}(\tau) = \lim_{t \rightarrow +\infty} \frac{\langle a_j^\dagger(t) a_i^\dagger(t+\tau) a_i(t+\tau) a_j(t) \rangle}{\langle a_j^\dagger(t) a_j(t) \rangle \langle a_i^\dagger(t+\tau) a_i(t+\tau) \rangle}, \quad (\text{S8})$$

where the expectation values are taken over the vacuum state. In the Schrödinger representation, this can be transformed to [61]

$$\begin{aligned} g_{ij}^{(2)}(\tau) &= \frac{\text{tr}[\bar{\rho} a_j^\dagger U^\dagger(\tau) a_i^\dagger a_i U(\tau) a_j]}{\bar{n}_i \bar{n}_j} \\ &= \frac{\text{tr}[U(\tau) \rho_j(0) U^\dagger(\tau) a_i^\dagger a_i]}{\bar{n}_i \bar{n}_j}, \end{aligned} \quad (\text{S9})$$

where  $U(\tau) = \exp(-i\mathcal{H}_{tot}\tau)$  is the time-evolution operator,  $\bar{\rho}$  is the steady state density operator, and  $\rho_j(0) \equiv a_j \bar{\rho} a_j^\dagger$ . In the denominator,  $\bar{n}_i \approx |\langle i|\bar{\psi}^{(1)}\rangle|^2 = |F_d G_{id}|^2$  under the weak drive approximation. The numerator can be calculated as  $\text{tr}[\rho_j(\tau) a_i^\dagger a_i]$ , where

$$\begin{cases} \rho_j(0) = a_j \bar{\rho} a_j^\dagger \\ \rho_j(\tau) = U(\tau) \rho_j(0) U^\dagger(\tau). \end{cases} \quad (\text{S10})$$

This is equivalent to calculating the  $i$ -th site's photon population at time  $\tau$ , using the modified initial state  $\rho_j(0)$ .

Now we convert the density operator back into the form  $\rho_j(\tau) \equiv |\psi_j(\tau)\rangle\langle\psi_j(\tau)|$ , and plug it into the numerator in Eq. (S9):

$$\text{tr}[U(\tau) \rho_j(0) U^\dagger(\tau) a_i^\dagger a_i] = \text{tr}[\rho_j(\tau) a_i^\dagger a_i] \approx |\langle i|\psi_j^{(1)}(\tau)\rangle|^2. \quad (\text{S11})$$

The Schrödinger equation corresponding to Eq. (S10) is

$$\begin{cases} |\psi_j(0)\rangle = a_j |\bar{\psi}\rangle \\ i \frac{d}{d\tau} |\psi_j(\tau)\rangle = \mathcal{H}_{tot} |\psi_j(\tau)\rangle. \end{cases} \quad (\text{S12})$$

We then recursively solve Eq. (S12) via Eq. (S2):

$$\begin{aligned} |\psi_j^{(k)}(0)\rangle &= a_j |\bar{\psi}^{(k+1)}\rangle, \\ i \frac{d}{d\tau} |\psi_j^{(k)}(\tau)\rangle &= \mathcal{H} |\psi_j^{(k)}(\tau)\rangle + \mathcal{H}_+ |\psi_j^{(k-1)}(\tau)\rangle. \end{aligned} \quad (\text{S13})$$

For the single-photon ( $k = 1$ ) subspace,

$$\begin{aligned} |\psi_j^{(1)}(0)\rangle &= a_j |\bar{\psi}^{(2)}\rangle, \\ i \frac{d}{d\tau} |\psi_j^{(1)}(\tau)\rangle &= \mathcal{H} |\psi_j^{(1)}(\tau)\rangle + F_d a_d^\dagger a_j |\bar{\psi}^{(1)}\rangle \\ &= \mathcal{H} |\psi_j^{(1)}(\tau)\rangle + F_d \langle j|\bar{\psi}^{(1)}\rangle |d\rangle, \end{aligned} \quad (\text{S14})$$

where we make use of the fact that  $|\psi_j^{(0)}(\tau)\rangle = |\psi_j^{(0)}(0)\rangle = a_j |\bar{\psi}^{(1)}\rangle$  is the vacuum state. The solution to Eq. (S14) is

$$|\psi_j^{(1)}(\tau)\rangle = |\psi_j^{(1)}(+\infty)\rangle + e^{-i\mathcal{H}\tau} [|\psi_j^{(1)}(0)\rangle - |\psi_j^{(1)}(+\infty)\rangle]. \quad (\text{S15})$$

The steady state  $|\psi_j^{(1)}(+\infty)\rangle$  can be obtained by setting the time derivative to zero in Eq. (S14):

$$\begin{aligned} 0 &= \mathcal{H} |\psi_j^{(1)}(+\infty)\rangle + F_d \langle j|\bar{\psi}^{(1)}\rangle |d\rangle, \\ |\psi_j^{(1)}(+\infty)\rangle &= -\mathcal{H}^{-1} F_d \langle j|\bar{\psi}^{(1)}\rangle |d\rangle = \langle j|\bar{\psi}^{(1)}\rangle |\bar{\psi}^{(1)}\rangle. \end{aligned} \quad (\text{S16})$$

The initial state  $|\psi_j^{(1)}(0)\rangle = a_j |\bar{\psi}^{(2)}\rangle$  is directly obtained by referring to Eq. (S6):

$$\begin{aligned} |\psi_j^{(1)}(0)\rangle &= a_j |\bar{\psi}^{(2)}\rangle = \langle j|\bar{\psi}^{(1)}\rangle |\bar{\psi}^{(1)}\rangle - \sqrt{2}\alpha F_d^2 \sum_{mnk} G_{kd}^2 \frac{\langle \varphi_{mn}|k, k\rangle \langle j|\varphi_m\rangle |\varphi_n\rangle + \langle j|\varphi_n\rangle |\varphi_m\rangle}{\sqrt{2}}, \\ &= \langle j|\bar{\psi}^{(1)}\rangle |\bar{\psi}^{(1)}\rangle - 2\alpha F_d^2 \sum_{mnk} \frac{G_{kd}^2 \langle \varphi_{mn}|k, k\rangle \langle j|\varphi_m\rangle}{2z + \epsilon_m + \epsilon_n} |\varphi_n\rangle. \end{aligned} \quad (\text{S17})$$

Finally, plugging Eq. (S17) and Eq. (S16) back into Eq. (S15) gives

$$\langle i|\psi_j^{(1)}(\tau)\rangle = \langle j|\bar{\psi}^{(1)}\rangle \langle i|\bar{\psi}^{(1)}\rangle - 2\alpha F_d^2 \sum_k G_{kd}^2 \langle i, j|G^{(2)}(\tau)|k, k\rangle, \quad (\text{S18})$$



where

$$G^{(2)}(\tau) \equiv \sum_{mn} \frac{|\varphi_{mn}\rangle\langle\varphi_{mn}|}{2z + \epsilon_m + \epsilon_n} e^{-i(z+\epsilon_n)\tau}. \quad (\text{S19})$$

We finally arrive at a perturbative solution for the delayed second-order correlation function:

$$g_{ij}^{(2)}(\tau) = \left| \frac{\langle i|\psi_j^{(1)}(\tau)\rangle^2}{\bar{n}_i\bar{n}_j} \right| = \left| \frac{\langle i|\psi_j^{(1)}(\tau)\rangle}{\langle i|\bar{\psi}^{(1)}\rangle\langle j|\bar{\psi}^{(1)}\rangle} \right|^2 \quad (\text{S20})$$

$$= \left| 1 - 2\alpha \sum_k \frac{G_{kd}^2}{G_{id}G_{jd}} \langle i, j|G^{(2)}(\tau)|k, k\rangle \right|^2. \quad (\text{S21})$$

## S2. CONVENTIONAL PHOTON BLOCKADE

To model conventional photon blockade model, we cannot use the perturbative procedure from the previous section, as  $\alpha$  is large. However, Eqs. (S9)–(S15) remain valid, and can be solved directly for a single-cavity system. In this case, the non-driven Hamiltonian is

$$\mathcal{H} = za_1^\dagger a_1 + \alpha a_1^\dagger a_1^\dagger a_1 a_1, \quad (\text{S22})$$

and the 1-photon and 2-photon Green's functions are

$$G = \frac{|1\rangle\langle 1|}{z}, \quad G^{(2)} = \frac{|1, 1\rangle\langle 1, 1|}{2z + 2\alpha}. \quad (\text{S23})$$

According to Eq. (S3), the steady state wavefunctions are

$$|\bar{\psi}^{(1)}\rangle = -\frac{F}{z}|1\rangle, \quad |\bar{\psi}^{(2)}\rangle = \frac{F^2}{\sqrt{2z(z+\alpha)}}|1, 1\rangle. \quad (\text{S24})$$

Plugging into Eqs. (S14) and Eq. (S15), we obtain

$$|\psi_1^{(1)}(0)\rangle = a_1|\bar{\psi}^{(2)}\rangle = \frac{F^2}{z(z+\alpha)}|1\rangle \quad (\text{S25})$$

$$|\psi_1^{(1)}(+\infty)\rangle = \frac{F^2}{z^2}|1\rangle \quad (\text{S26})$$

$$\Rightarrow |\psi_1^{(1)}(\tau)\rangle = \frac{F^2}{z^2} \left( 1 - \frac{\alpha}{\alpha+z} e^{-iz\tau} \right) |1\rangle. \quad (\text{S27})$$

Thus, the second-order correlation function is

$$g_{11}^{(2)}(\tau) = \left| \frac{\langle 1|\psi_1^{(1)}(\tau)\rangle}{\langle 1|\bar{\psi}^{(1)}\rangle^2} \right|^2 = \left| 1 - \frac{\alpha}{\alpha+z} e^{-iz\tau} \right|^2. \quad (\text{S28})$$

Optimal parameters for photon blockade can be found by minimizing the equal-time second-order correlation:

$$g_{11}^{(2)}(0) = \left| \frac{z}{\alpha+z} \right|^2 = \frac{\Delta^2 + \frac{\gamma^2}{4}}{(\Delta+\alpha)^2 + \frac{\gamma^2}{4}}, \quad (\text{S29})$$

$$\Delta_{min} = -\frac{1}{2}(\alpha - \sqrt{\alpha^2 + \gamma^2}). \quad (\text{S30})$$

For large nonlinearity  $\alpha \gg \gamma$ , we can achieve  $\Delta_{min} \approx 0$ , and the corresponding time-delayed correlation function is

$$g_{11}^{(2)}(\tau) = 1 - \frac{4\alpha^2(2e^{-\frac{\gamma}{2}\tau} - e^{-\gamma\tau})}{4\alpha^2 + \gamma^2} \quad (\text{S31})$$

$$= \frac{\gamma^2}{4\alpha^2 + \gamma^2} + \frac{4\alpha^2}{4\alpha^2 + \gamma^2} \left( 1 - e^{-\frac{\gamma}{2}\tau} \right)^2 \quad (\text{S32})$$

$$\approx \left( 1 - e^{-\frac{\gamma}{2}\tau} \right)^2. \quad (\text{S33})$$

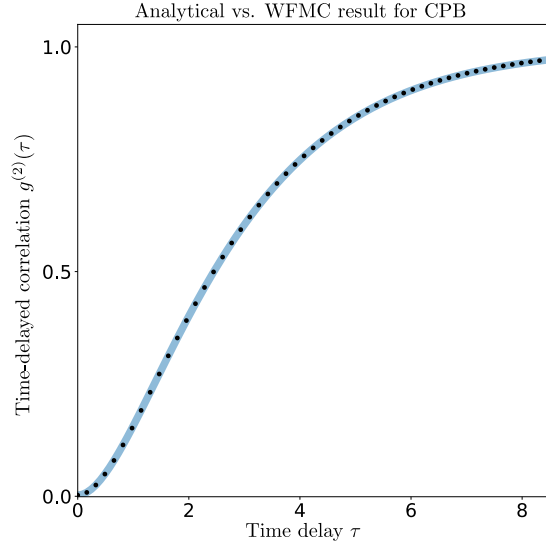


FIG. S1. Time-delayed correlation function  $g_{11}^{(2)}(\tau)$  for conventional photon blockade in a single cavity, using the analytical result (S32) (solid blue line) and WPMC simulations (black dots). The system parameters are the same as in the conventional blockade system from Fig. 2 of the main text.

Fig. S1 shows an exemplary plot of  $g_{11}^{(2)}(\tau)$  versus  $\tau$ , comparing Eq. (S32) (solid blue curve) to wavefunction Monte Carlo (WPMC) simulations (black dots). The theoretical results are clearly very accurate.

### S3. UNCONVENTIONAL PHOTON BLOCKADE IN TWO CAVITIES

In this section, we re-derive unconventional photon blockade (UPB) in a two-cavity system using the framework of Section S1. Here, the coupling Hamiltonian is

$$[J_{ij}] = \begin{pmatrix} 0 & J \\ J & 0 \end{pmatrix}, \quad (\text{S34})$$

and its eigenvectors and eigenvalues are

$$(|\varphi_1\rangle \quad |\varphi_2\rangle) = \frac{1}{\sqrt{2}} \begin{pmatrix} -1 & 1 \\ 1 & 1 \end{pmatrix}, \quad \begin{pmatrix} \epsilon_1 \\ \epsilon_2 \end{pmatrix} = \begin{pmatrix} -J \\ J \end{pmatrix}. \quad (\text{S35})$$

As in the original UPB model [29–31], we drive and measure at cavity 1. From Eq. (S21),

$$g_{ij}^{(2)}(\tau) = \left| 1 - 2\alpha e^{-iz\tau} \sum_n A_{ij}(n) e^{-i\epsilon_n \tau} \right|^2, \quad (\text{S36})$$

$$A_{ij}(n) = \sum_{km} \frac{G_{kd}^2}{G_{id}G_{jd}} \frac{\langle i, j | \varphi_{mn} \rangle \langle \varphi_{mn} | k, k \rangle}{2z + \epsilon_m + \epsilon_n}. \quad (\text{S37})$$

By inserting Eq. (S35) into Eq. (S37) (note that  $G = \sum_n (z + \epsilon_n)^{-1} |\varphi_n\rangle \langle \varphi_n|$ ), we have

$$A_{11}(1) = \frac{2z^3 - Jz^2 + J^3}{8z^3(z - J)}, \quad A_{11}(2) = -\frac{2z^3 + Jz^2 - J^3}{8z^3(z + J)}. \quad (\text{S38})$$

Hence the interfered oscillation terms sum up to

$$\sum_n A_{11}(n) e^{-i\epsilon_n \tau} = \frac{2z^4 - J^2 z^2 + J^4}{4z^3(z^2 - J^2)} \cos J\tau + i \frac{Jz(z^2 + J^2)}{4z^3(z^2 - J^2)} \sin J\tau. \quad (\text{S39})$$

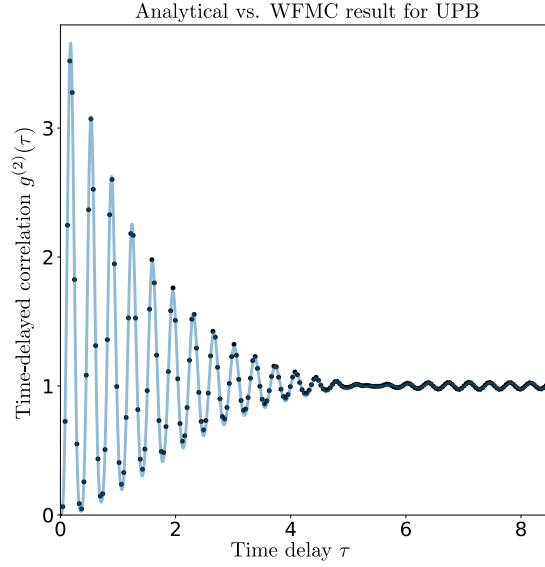


FIG. S2. Time-delayed correlation function  $g_{11}^{(2)}(\tau)$  for UPB in a two-cavity system, showing analytical results (solid blue curve) and WFCM simulation results (black dots). The system parameters are the same as in Fig. 2 of the main text.

The optimal antibunching condition is

$$g_{11}^{(2)}(0) = \left| 1 - 2\alpha \cdot \frac{2z^4 - J^2z^2 + J^4}{4z^3(z^2 - J^2)} \right|^2 = 0. \quad (\text{S40})$$

This can be satisfied for weak nonlinearity (i.e., small  $\alpha$ ) by taking  $J$  to be large, so that

$$z = \Delta - \frac{i}{2}\gamma \approx \left( \frac{\alpha J^2}{2} \right)^{\frac{1}{3}} e^{-\frac{i\pi}{3}}. \quad (\text{S41})$$

This is consistent with the results of earlier studies, such as Ref. [31]. The corresponding delayed second-order correlation function is

$$\begin{aligned} g_{11}^{(2)}(\tau) &= \left| 1 - e^{-iz\tau} \cos J\tau + iO(\alpha^{\frac{1}{3}}) \right|^2 \\ &\approx \left| 1 - e^{-\frac{\gamma}{2}\tau} e^{-i\Delta\tau} \cos J\tau \right|^2 \\ &\approx \left( 1 - e^{-\frac{\gamma}{2}\tau} \cos \Delta\tau \cos J\tau \right)^2. \end{aligned} \quad (\text{S42})$$

In the last line, we have used the fact that  $\Delta \ll J$  since  $(\Delta/J)^3 \approx (1/16)\alpha/J \ll 1$ , and the imaginary part of the slow-varying  $e^{-i\Delta\tau}$  can be omitted. In Fig. S2, we compare this analytical formula to WFCM simulation results, using the same UPB settings as in Fig. 2 of the main text.

#### S4. LONG-LIVED PHOTON BLOCKADE

As discussed in the main text, our desired route to photon blockade is to find a situation where  $G_{ij} = 0$  at a large value of the cavity decay rate (relative to the coupling strength). Let us consider a more general scenario than in the main text, whereby all the couplings  $J_{ij}$  and the complex detunings  $z_i$  are independently tunable. For the two-cavity system, we have

$$\mathcal{H} = \begin{pmatrix} z_1 & J \\ J & z_2 \end{pmatrix}, \quad G = \frac{1}{z_1 z_2 - J^2} \begin{pmatrix} z_2 & -J \\ -J & z_1 \end{pmatrix}. \quad (\text{S43})$$

Clearly, if  $J$  is non-vanishing, a zero of  $G$  is only achievable for  $z_1 = 0$  or  $z_2 = 0$ , which does not meet our requirements.

For three cavities,

$$\mathcal{H} = \begin{pmatrix} z_1 & J_1 & J_3 \\ J_1 & z_2 & J_2 \\ J_3 & J_2 & z_3 \end{pmatrix}, \quad G = \frac{1}{z_1 z_2 z_3 - z_1 J_2^2 - z_2 J_3^2 - z_3 J_1^2 + 2J_1 J_2 J_3} \begin{pmatrix} z_2 z_3 - J_2^2 & J_2 J_3 - z_3 J_1 & J_1 J_2 - z_2 J_3 \\ J_2 J_3 - z_3 J_1 & z_3 z_1 - J_3^2 & J_3 J_1 - z_1 J_2 \\ J_1 J_2 - z_2 J_3 & J_3 J_1 - z_1 J_2 & z_1 z_2 - J_1^2 \end{pmatrix}. \quad (\text{S44})$$

There are two cases to consider. (i) To create a zero on the diagonal, two complex detunings must be conjugates of each other (e.g.,  $z_2 = z_3^*$  and  $|z_2| = |z_3| = J_2$ ). This requires either that one cavity has gain precisely balanced with another cavity's loss, or that both cavities are lossless. (ii) To create a zero off-diagonal entry, one complex detuning must be real (e.g.,  $z_3 = J_2 J_3 / J_1$ ), implying that the cavity must be completely lossless. Either requirement is somewhat impractical (though not impossible) compared to the four-cavity setup.

Let us now analyze the four-cavity system, shown schematically in Fig. 1(b) of the main text.

First, we will develop some intuition about how photon antibunching arises in this system. In the Dyson series expansion for  $G_{id}(z)$ , each term in the series can be interpreted as a photon trajectory starting at the driven cavity  $d$  and ending at the output cavity  $i$  [54]. Along a trajectory, each cavity contributes  $1/z$  to the Green's function. For  $G_{21}$ , the Dyson series up to order  $1/z^4$  has five terms, corresponding to the following trajectories:

Trajectory	Dyson series term
$1 \mapsto 2$	$\frac{1}{z} \cdot J_{12} \cdot \frac{1}{z}$
$1 \mapsto 2 \mapsto 1 \mapsto 2$	$\frac{1}{z} \cdot J_{12} \cdot \frac{1}{z} \cdot J_{12} \cdot \frac{1}{z} \cdot J_{12} \cdot \frac{1}{z}$
$1 \mapsto 2 \mapsto 3 \mapsto 2$	$\frac{1}{z} \cdot J_{12} \cdot \frac{1}{z} \cdot J_{23} \cdot \frac{1}{z} \cdot J_{23} \cdot \frac{1}{z}$
$1 \mapsto 4 \mapsto 1 \mapsto 2$	$\frac{1}{z} \cdot J_{41} \cdot \frac{1}{z} \cdot J_{41} \cdot \frac{1}{z} \cdot J_{12} \cdot \frac{1}{z}$
$1 \mapsto 4 \mapsto 3 \mapsto 2$	$\frac{1}{z} \cdot J_{41} \cdot \frac{1}{z} \cdot J_{34} \cdot \frac{1}{z} \cdot J_{23} \cdot \frac{1}{z}$

If we take the sum of these terms and equating it zero, we arrive at the following solution:

$$z = \pm i \sqrt{J_{41}^2 + J_{12}^2 + J_{23}^2 + \frac{J_{41} J_{23} J_{34}}{J_{12}}}. \quad (\text{S45})$$

When  $J_{12} \ll J_{41}, J_{23}, J_{34}$ , this solution is self-consistent as  $\gamma = -2\text{Im}(z) \approx 2\sqrt{J_{41} J_{23} J_{34} / J_{12}}$  is indeed larger than all the coupling terms.

Having established the feasibility of LLPB in this system, let us consider the simplified case  $J'/J \ll 1$ , which locates the pole at  $z_0 = -iJ\sqrt{k - J^2/J^2} \approx -iJ\sqrt{k}$  and  $\gamma \approx 2\sqrt{k}J$ . Then the eigenvectors and eigenvalues of the coupling Hamiltonian  $[J_{ij}]$  can be analytically written as second-order perturbation of  $J'$ :

$$(|\varphi_1\rangle |\varphi_2\rangle |\varphi_3\rangle |\varphi_4\rangle) = \frac{1}{2} \begin{pmatrix} -1 & -1 & 1 & 1 \\ 1 & -1 & -1 & 1 \\ -1 & 1 & -1 & 1 \\ 1 & 1 & 1 & 1 \end{pmatrix} + \frac{J'}{8J} \begin{pmatrix} 1 - \frac{1}{k} + \frac{J'}{8J} & -1 + \frac{1}{k} + \frac{J'}{8J} & 1 - \frac{1}{k} - \frac{J'}{8J} & -1 + \frac{1}{k} - \frac{J'}{8J} \\ -1 + \frac{1}{k} - \frac{J'}{8J} & -1 + \frac{1}{k} + \frac{J'}{8J} & -1 + \frac{1}{k} + \frac{J'}{8J} & -1 + \frac{1}{k} - \frac{J'}{8J} \\ -1 + \frac{1}{k} + \frac{J'}{8J} & -1 + \frac{1}{k} - \frac{J'}{8J} & 1 - \frac{1}{k} + \frac{J'}{8J} & 1 - \frac{1}{k} - \frac{J'}{8J} \\ 1 - \frac{1}{k} - \frac{J'}{8J} & -1 + \frac{1}{k} - \frac{J'}{8J} & -1 + \frac{1}{k} - \frac{J'}{8J} & 1 - \frac{1}{k} - \frac{J'}{8J} \end{pmatrix}, \quad (\text{S46})$$

$$\begin{pmatrix} \epsilon_1 \\ \epsilon_2 \\ \epsilon_3 \\ \epsilon_4 \end{pmatrix} = J \begin{pmatrix} -1 \\ -1 \\ 1 \\ 1 \end{pmatrix} + \frac{J'}{2} \begin{pmatrix} -1 - \frac{1}{k} - \frac{J'}{4J} \\ 1 + \frac{1}{k} - \frac{J'}{4J} \\ -1 - \frac{1}{k} + \frac{J'}{4J} \\ 1 + \frac{1}{k} + \frac{J'}{4J} \end{pmatrix}. \quad (\text{S47})$$

The single photon Green's function to the second order of  $J'/J$  are given by

$$G = \begin{pmatrix} \frac{J^2 J'^2 z}{(z^2 - J^2)^3} + \frac{z}{z^2 - J^2} & -\frac{J' z^2}{k(J^2 - z^2)^2} - \frac{J^2 J'}{(J^2 - z^2)^2} & \frac{J J' z}{k(J^2 - z^2)^2} + \frac{J J' z}{(J^2 - z^2)^2} & \frac{J J'^2 z^2}{(J^2 - z^2)^3} + \frac{J}{J^2 - z^2} \\ -\frac{J' z^2}{k(J^2 - z^2)^2} - \frac{J^2 J'}{(J^2 - z^2)^2} & \frac{J^2 J'^2 z}{(z^2 - J^2)^3} + \frac{z}{z^2 - J^2} & \frac{J J'^2 z^2}{(J^2 - z^2)^3} + \frac{J}{J^2 - z^2} & \frac{J J' z}{k(J^2 - z^2)^2} + \frac{J J' z}{(J^2 - z^2)^2} \\ \frac{J J' z}{k(J^2 - z^2)^2} + \frac{J J' z}{(J^2 - z^2)^2} & \frac{J J'^2 z^2}{(J^2 - z^2)^3} + \frac{J}{J^2 - z^2} & \frac{J'^2 z^3}{(z^2 - J^2)^3} + \frac{z}{z^2 - J^2} & -\frac{J^2 J'}{k(J^2 - z^2)^2} - \frac{J' z^2}{(J^2 - z^2)^2} \\ \frac{J J'^2 z^2}{(J^2 - z^2)^3} + \frac{J}{J^2 - z^2} & \frac{J J' z}{k(J^2 - z^2)^2} + \frac{J J' z}{(J^2 - z^2)^2} & -\frac{J^2 J'}{k(J^2 - z^2)^2} - \frac{J' z^2}{(J^2 - z^2)^2} & \frac{J'^2 z^3}{(z^2 - J^2)^3} + \frac{z}{z^2 - J^2} \end{pmatrix}. \quad (\text{S48})$$

Let  $G_{12} = 0$ , we get the pole  $z_0 = -i\sqrt{k}J$ . Expanding  $z$  near the pole as  $z = z_0 + \delta z$ , plugging the eigenvectors, eigenvalues and Green's function into Eq. (S37), we get:

$$2\alpha \sum_n A_{22}(n)e^{-i\epsilon_n\tau} \approx \frac{i\alpha J}{1024\delta z^2} \left\{ \cos(J\tau) \left[ 16J\tau(-3k^2 - 10k) - 304\sqrt{k} + 3\frac{J'^2\tau}{J}k^3 \right] + \sin(J\tau) \left[ 48k^2 - 144k - 3\frac{J'^2\tau}{J}k^{5/2} - 3\frac{J'^2}{J^2}k^3 \right] \right\}. \quad (\text{S49})$$

Requiring  $g_{22}^{(2)}(0) = 0$  gives

$$-\frac{19i\alpha\sqrt{k}J}{64\delta z^2} = 1 \Rightarrow \delta z = \pm \frac{\sqrt{19}}{8}k^{1/4}\sqrt{\alpha J}e^{-\pi i/4}. \quad (\text{S50})$$

Hence, Eq.(S49) becomes

$$2\alpha \sum_n A_{22}(n)e^{-i\epsilon_n\tau} \approx \frac{\sqrt{k}}{304} \left\{ \cos(J\tau) \left[ 16J\tau(3k + 10) + \frac{304}{\sqrt{k}} - 3\frac{J'^2\tau}{J}k^2 \right] + 3\sin(J\tau) \left[ 48 - 16k + \frac{J'^2\tau}{J}k^{3/2} + \frac{J'^2}{J^2}k^2 \right] \right\}. \quad (\text{S51})$$

The comparison between Eq. (S51) and WFMC results are shown in Fig. S3.

In the short timescales  $J\tau \ll 1$ ,

$$2\alpha \sum_n A_{22}(n)e^{-i\epsilon_n\tau} \approx 1 + \sqrt{k}J\tau + \frac{-152 + 3J'^2k^2/J^2}{304}J^2\tau^2 \quad (\text{S52})$$

The correlation function  $g_{22}^{(2)}(\tau)$  is then given by Eq. (S36) with  $z$  given by  $z = z_0 + \delta z$ . In the short timescales  $J\tau \ll 1$ ,  $g_{22}^{(2)}(\tau)$  behaves as

$$g_{22}^{(2)}(\tau) = \left| 1 - 2\alpha e^{-iz\tau} \sum_n A_{22}(n)e^{-i\epsilon_n\tau} \right|^2 \approx \left| \frac{(1+i)\sqrt{19}}{8\sqrt{2}} \sqrt{\frac{\alpha}{J}}k^{1/4}J\tau + \frac{1}{128} \left( 64k - 19i\frac{\alpha}{J}\sqrt{k} \right) J^2\tau^2 \right|^2. \quad (\text{S53})$$

If we assume negligible nonlinearity  $\alpha/J \ll 1$  and thus  $\gamma = -2\text{Im}\{z\} \approx -2\text{Im}\{z_0\} = 2\sqrt{k}J$ , the result can be further approximated as

$$g_{22}^{(2)}(\tau) \approx \left| \frac{1}{2}kJ^2\tau^2 \right|^2 \approx (\gamma\tau)^4/64. \quad (\text{S54})$$

## S5. EQUAL-TIME SECOND ORDER CORRELATION VS. PHOTON OCCUPATION NUMBER

This section looks into the dependence of the equal-time second order correlation on photon occupation in the signal cavity. Due to the weak coupling  $J'/k$  between the driven cavity and signal cavity, the photon number in the driven cavity is several orders of magnitude larger than in the signal cavity, making the WFMC simulation with high signal cavity photon occupation difficult.

To overcome this problem and demonstrate the  $g^{(2)}(\tau)$  dependence on photon occupation  $n$ , we use another set of parameters with  $k = 4$  instead of  $k = 16$ , and  $J' = J = 0.5386$  instead of  $J' = 0.2J$ . The other parameters are  $\gamma = 1$ ,  $\alpha = 0.0194$  and  $\Delta = 0.0652$ . Fig. S4(a) shows the resulting comparison between the LLPB system, the two-cavity UPB model (with the same  $\gamma$  and  $\alpha$ ), and a conventional photon blockade system (with the same  $\gamma$  and large  $\alpha = 10$ ). The enlarged antibunching time window and the flat bottom near  $\tau = 0$  can still be observed. Fig. S4(b) then shows the equal-time second order correlation versus the photon occupation number in the signal cavity.

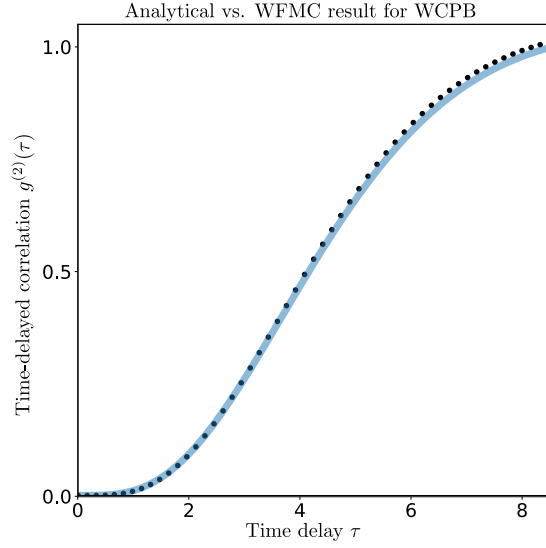


FIG. S3. Time-delayed correlation function  $g_{22}^{(2)}(\tau)$  for weak-coupling photon blockade in a four-cavity system, using the full analytical formula (S51) (solid blue curve), and WFCM simulations (black dash). The system parameters are the same as in Fig. 2 of the main text.

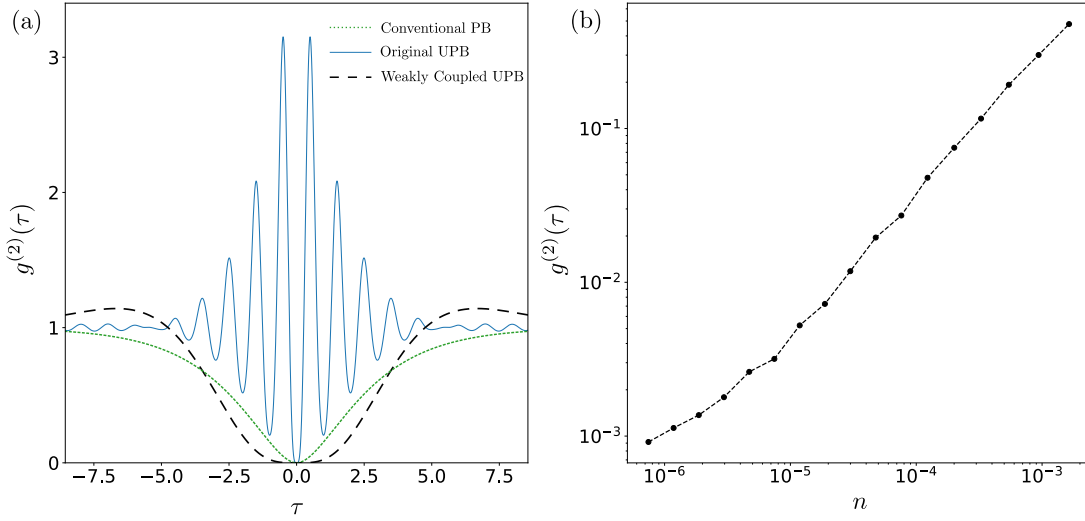


FIG. S4. WFCM simulations of the weakly coupled UPB model for another parameter setup with  $k = 4$ ,  $\gamma = 1$ ,  $J' = J = 0.5386$ ,  $\alpha = 0.0194$  and  $\Delta = 0.0652$ . (a) Comparison with conventional photon blockade and original UPB models. (b) Signal cavity photon occupation number versus equal-time second order correlation.